

Room Temperature Synthesis and Characterization of Novel Lead-free Double Perovskite Nanocrystals with a Stable and Broadband Emission

Yingying Tang,^a Leyre Gomez,^{a,b} Marco van der Laan,^a Dolf Timmerman,^c Victor Sebastian,^{d,e,f} Chia-Ching Huang,^a Tom Gregorkiewicz,^a and Peter Schall ^{*a}

a. Institute of Physics, University of Amsterdam, Science Park 904, 1098 XH Amsterdam, The Netherlands

b. Catalan Institute of Nanoscience and Nanotechnology, CSIC, BIST, and CIBER BBN, 08193 Bellaterra Barcelona, Spain

c. Graduate School of Engineering, Osaka University, 2-1 Yamadaoka, Suita, Osaka 565-0871, Japan

d. Department of Chemical Engineering and Environmental Technology, Universidad de Zaragoza, Campus Río Ebro-Edificio I+D, 50018 Zaragoza, Spain

e. Instituto de Nanociencia y Materiales de Aragón (INMA), University of Zaragoza-CSIC, c/ María de Luna 3, 50018 Zaragoza, Spain

f. Networking Research Center on Bioengineering Biomaterials and Nanomedicine (CIBER- BBN), Madrid, Spain

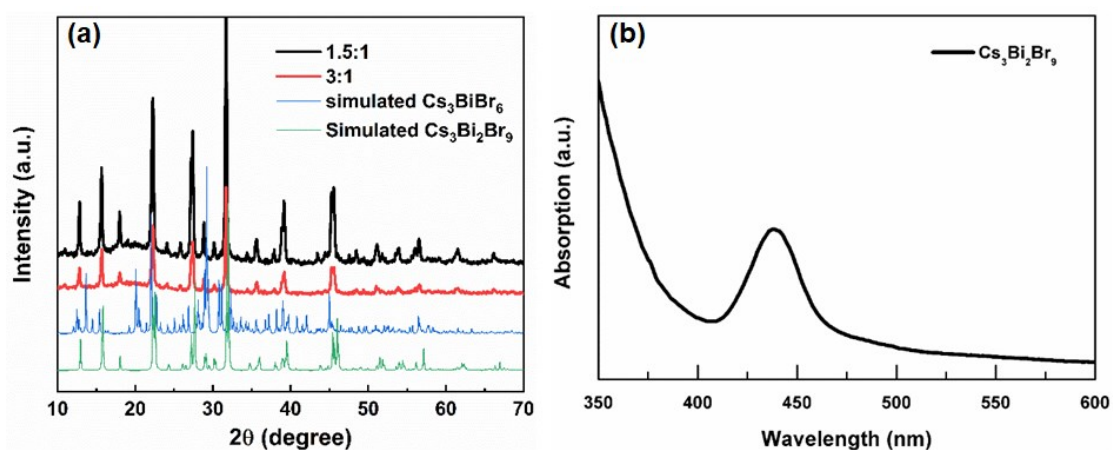


Fig. S1. (a) XRD patterns for precursor ratios of CsBr and BiBr₃ at 1.5:1 and 3:1 compared to simulated Cs₃Bi₂Br₉ and Cs₃BiBr₆ XRD pattern. (b) UV spectra of the Cs₃Bi₂Br₉ NCs.

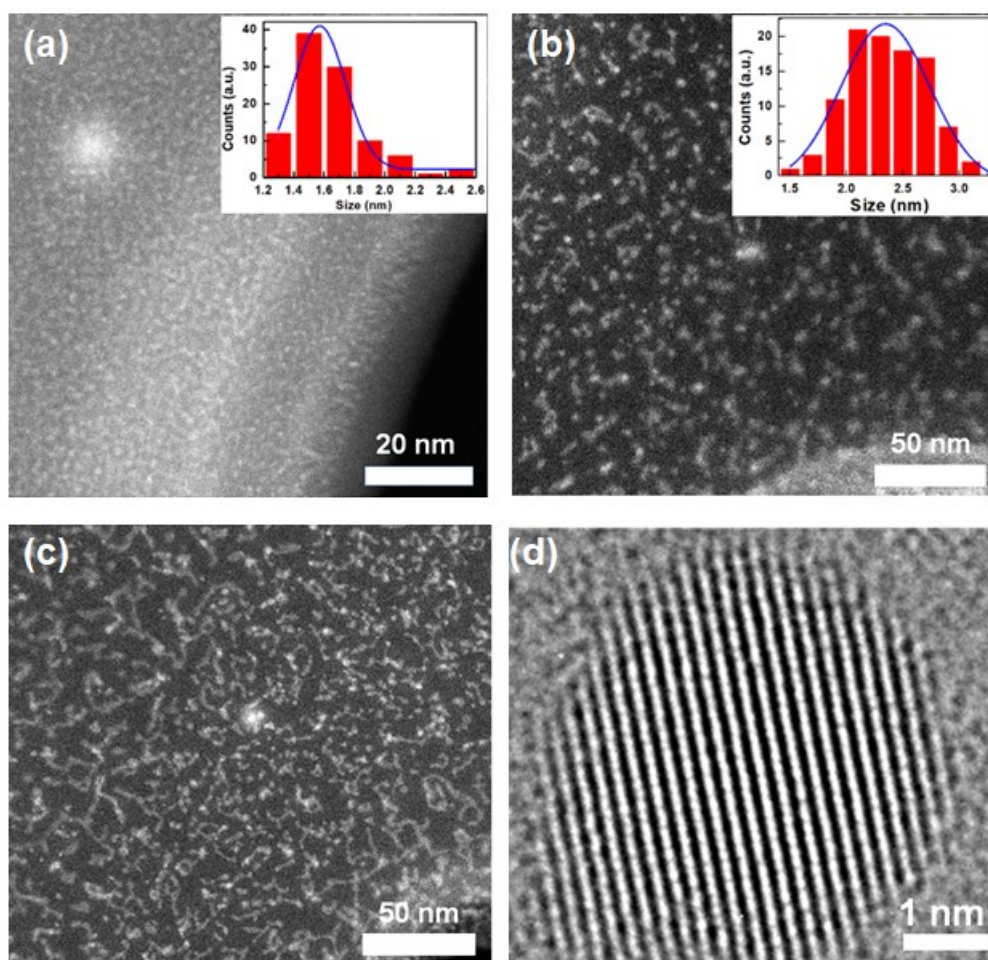


Fig. S2. (a) HAADF-STEM image for Cs₃BiBr_{6-5.5} NCs, the inset is the size distribution. (b) HAADF-STEM image for Cs₃BiBr₆₋₁₀ NCs, the inset is the size distribution. (c) HAADF-STEM image for Cs₃BiBr₆₋₁₀ NCs. (d) HRTEM image for Cs₃BiBr₆₋₁₀ NC with a lattice fringe of 0.22 nm.

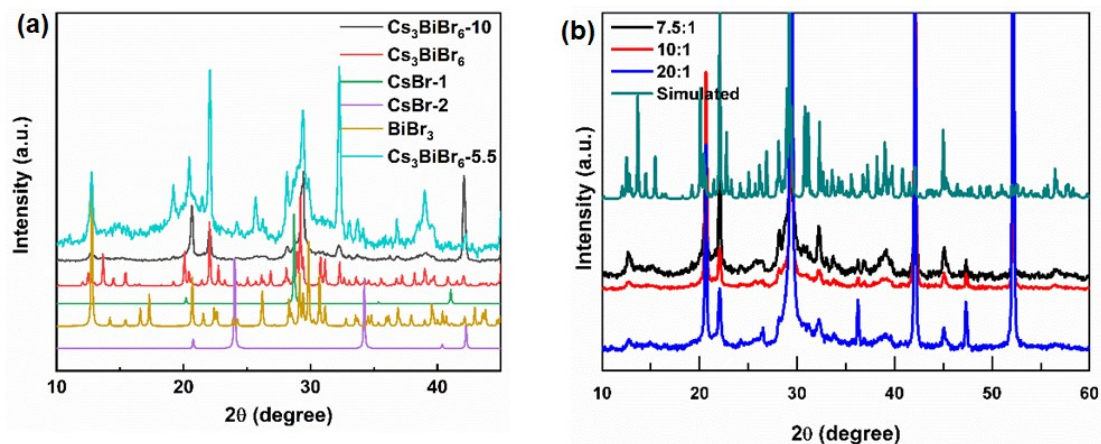


Fig. S3. (a) Comparison of XRD patterns with the simulated XRD patterns of precursors (CsBr-1 , $Fm-3m$; CsBr-2 , $Pm-3m$; BiBr_3 , $P2_1/c$), Cs_3BiBr_6 and $\text{Cs}_3\text{BiBr}_6\text{-5.5}$ NCs. (b) Zoom-in of the XRD pattern of $\text{Cs}_3\text{BiBr}_6\text{-7.5}$, $\text{Cs}_3\text{BiBr}_6\text{-10}$, $\text{Cs}_3\text{BiBr}_6\text{-20}$ NCs.

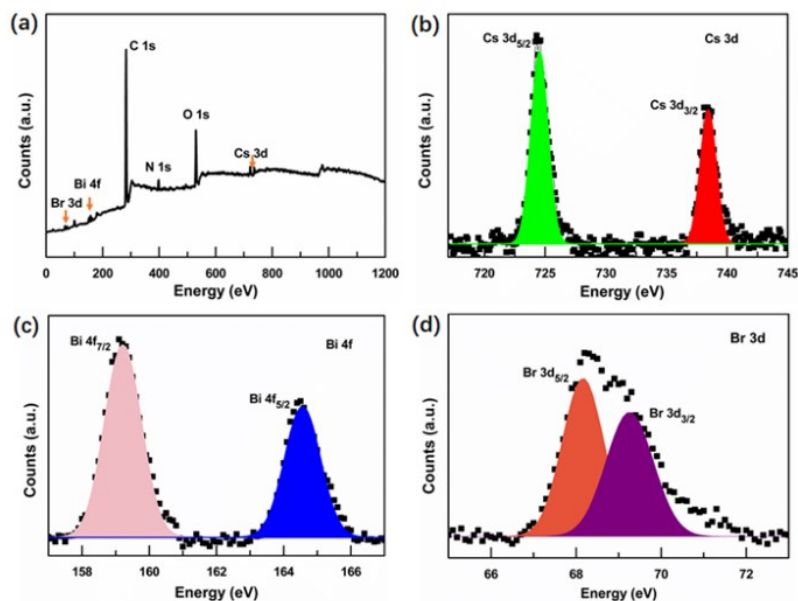


Fig. S4. XPS characteristics for $\text{Cs}_3\text{BiBr}_6\text{-5.5}$ NCs: (a) Survey spectra; (b) Cs 3d; (c) Bi 4f; (d) Br 3d. For Cs 3d electrons, the two peaks centred at 724.4 eV and 738.4 eV correspond to the Cs 3d_{5/2} and Cs 3d_{3/2} states with a spin-orbit splitting of 14 eV. Similarly, in the Br 3d spectra, peaks at 68.1 eV and 69.3 eV are assigned to Br 3d_{5/2} and Br 3d_{3/2}, with a well-resolved spin-orbit splitting of ~ 1.2 eV, while in the Bi 4f spectra, two peaks located at 159.2 eV and 164.6 eV, with a spin-orbit splitting of 5.4 eV, can be observed.

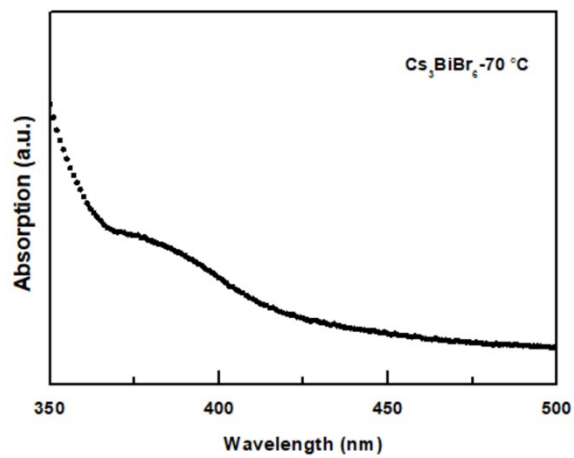


Fig. S5. Absorption spectra for Cs₃BiBr₆ NCs synthesized at 70 °C.

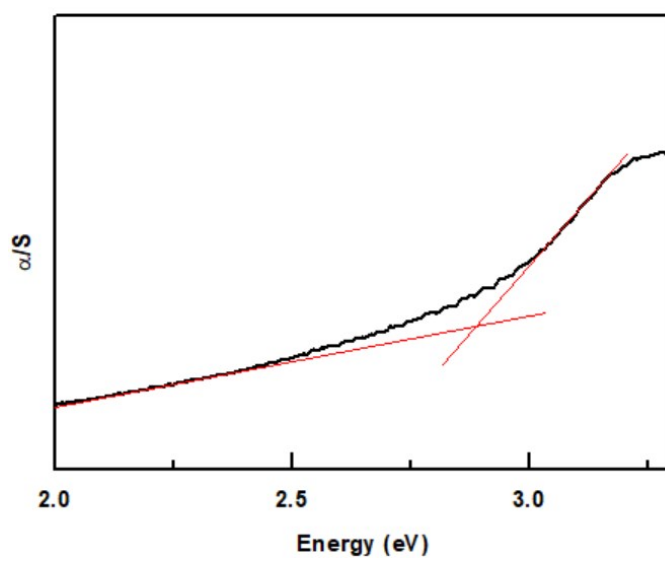


Fig. S6. Tauc' plot for Cs₃BiBr₆ NCs.

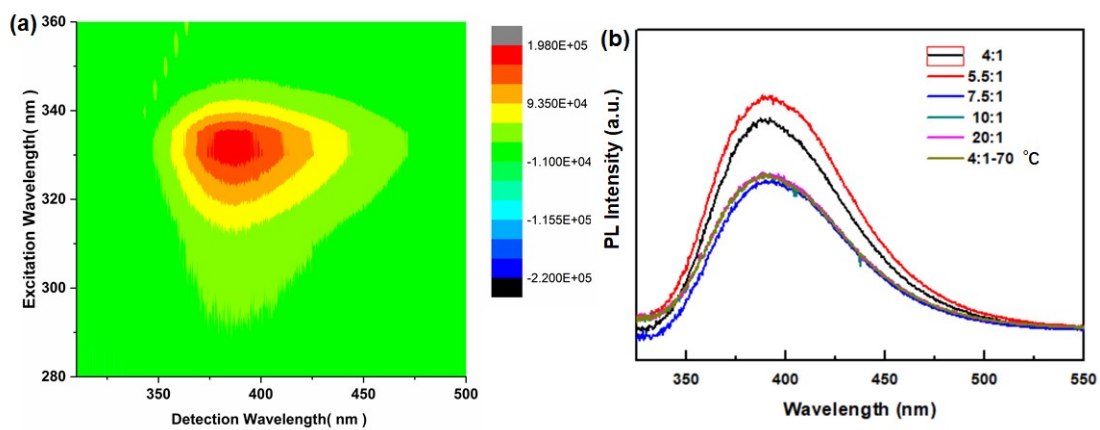


Fig. S7. (a) PL contour map for OA ligands. (b) Cs_3BiBr_6 NCs with OA ligands.

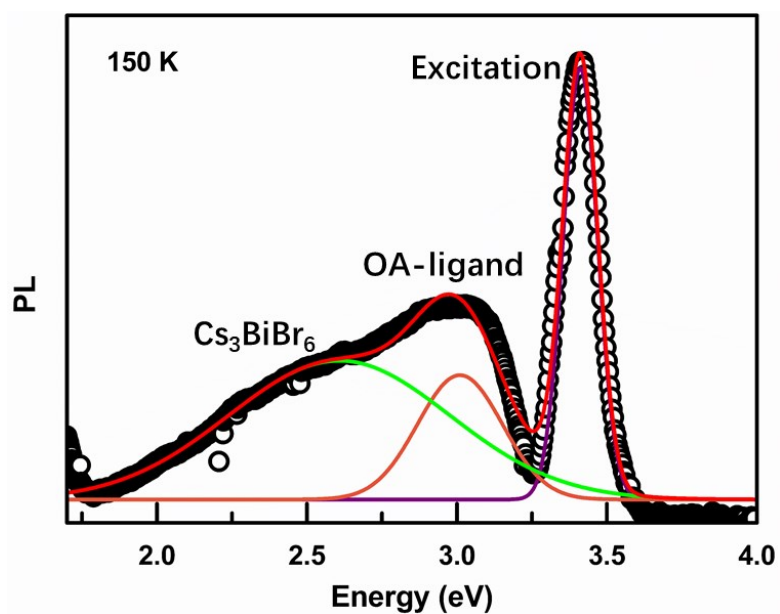


Fig. S8. Gaussian fitting with three peaks: excitation peak, OA-ligand related peak and Cs_3BiBr_6 -related emission for PL emission of Cs_3BiBr_6 NCs at 150 K.

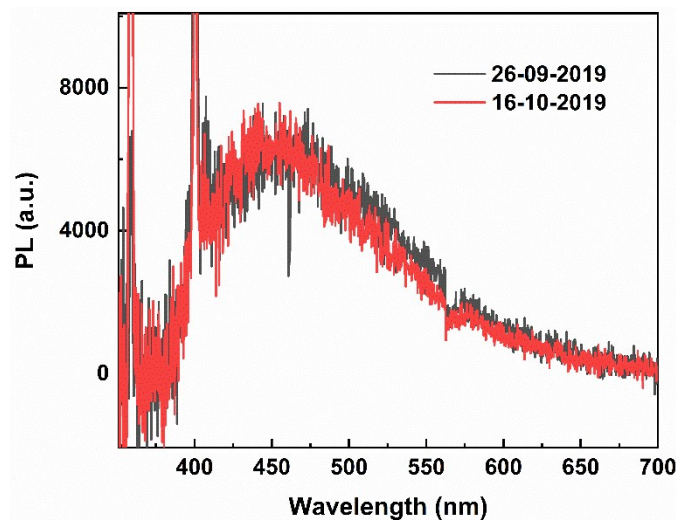


Fig. S9. PL spectra for Cs_3BiBr_6 NCs at room temperature before and after three weeks by an excitation wavelength of 355 nm.

Table S1. Crystal data and structure refinements for the Cs_3BiBr_6 at 120 K.

| formula | Cs_3BiBr_6 |
|--|----------------------------|
| fw | 1087.17 |
| T, K | 120 K |
| λ , Å | 0.71073 |
| Space group | <i>Pbcm</i> |
| a, Å | 8.637(3) |
| b Å | 13.495(6) |
| c, Å | 27.532(6) |
| α , deg | 90 |
| β , deg | 90 |
| γ , deg | 90 |
| V, Å ³ | 3209.3(5) |
| Z | 8 |
| D_{calcd} , g cm ⁻³ | 4.500 |
| μ , mm ⁻¹ | 32.59 |
| GOF on F ² | 1.345 |
| R1, wR2[$I > 2\sigma(I)$] ^a | 0.0691, 0.1703 |
| R1, wR2(all data) | 0.0806, 0.1745 |